energy&fuels

Article

pubs.acs.org/EF

# Pyrolysis and Combustion Behavior of Coal Gangue in $O_2/CO_2$ and $O_2/N_2$ Mixtures Using Thermogravimetric Analysis and a Drop Tube Furnace

Fanrui Meng,[†] Jianglong Yu,*[,†,‡] Arash Tahmasebi,[†] and Yanna Han[†]

[†]Key Laboratory of Advanced Coal and Coking Technology of Liaoning Province, School of Chemical Engineering, University of Science and Technology Liaoning, Anshan (114051), P.R. China

[‡]Thermal Energy Research Centre, Shenyang Aerospace University, Shenyang (110136), P.R. China

**ABSTRACT:** Combustion of coal gangue is extensively used for power generation in China. In this paper, pyrolysis and combustion characteristics of a low-rank coal gangue have been investigated under oxy-fuel ($O_2/CO_2$) and air ($N_2/O_2$) conditions using a drop tube furnace and thermogravimetric analysis. Pyrolysis experiments were carried out in $N_2$ and $CO_2$ environments, which are the main diluting gases of air and oxy-fuel environments, respectively. The burnout and yields of volatile matter were analyzed during DTF experiments. At lower temperatures, the weight loss rate of coal gangue during pyrolysis in $N_2$ was higher than that in $CO_2$. However, further weight loss took place in $CO_2$ atmosphere at temperatures above 800 °C due to $CO_2$ gasification of chars. The thermogravimetric analysis (TGA) results confirmed that the pyrolysis in $CO_2$ environment can be divided into three stages: moisture release, devolatilization, and char gasification by $CO_2$ in a higher temperature zone. Combustion experiments were carried out in four different atmospheres: air, an oxygen-enriched air environment (30% $O_2$−70% $N_2$ and 40% $O_2$−60% $N_2$), an oxy-fuel environment (21% $O_2$−79% $CO_2$), and an oxygen-enriched oxy-fuel environment (30% $O_2$−70% $CO_2$ and 40% $O_2$−60% $CO_2$). Coal gangue reactivity under oxy-fuel conditions differed from that under air combustion conditions. The combustion rate of coal gangue increased with increasing $O_2$ concentration while the ignition and burnout points shifted to lower temperatures and complete combustion was achieved at lower temperatures and shorter times. Comparison of the combustion performance of coal gangue in $N_2/O_2$ and $CO_2/O_2$ environments for equivalent $O_2$ concentrations indicated that the combustion characteristics of coal gangue in a $CO_2/O_2$ environment were similar to those in a $N_2/O_2$ environment at 21 vol % $O_2$ oxygen concentrations. However, increasing $O_2$ partial pressures resulted in a higher combustion rate under oxy-fuel conditions. Kinetic constants for the samples were calculated by using the isoconventional method. The activation energy decreased with increasing $O_2$ partial pressure under oxy-fuel combustion conditions and reached lower values compared to air combustion cases. The mineral matter reactions during coal gangue combustion were investigated by means of XRD analysis. During combustion at 1200 °C, mineral phases in coal gangue were transformed to ash comprised of kaolinite, quartz, mullite, magnetite, hematite, and anhydrite.

## 1. INTRODUCTION

Coal gangue is extensively utilized as a low-grade energy source for power generation in China that heavily relies on coal to supply energy. China has become the largest coal producer and consumer in the world due to the increasing demand on coal to generate electricity.[1] A large amount of coal gangue is being produced every year as a consequence of increasing coal mining and processing. The gangue accounts for approximately 10%−15% of the amount of coal produced.[1] Coal gangue occupies land, and its spontaneous combustion and leaching result in serious pollution of air, water, and soil.[2−4] Therefore, coal gangue utilization is of utmost concern and has attracted wide interest in China, including for use in power generation[5,6] and construction materials.[5,7,8]

Oxy-fuel combustion is one of the most promising technologies for carbon capture and storage that is undergoing rapid development in recent years.[9,10] The $CO_2$ gas is more dense and has a higher specific heat capacity than $N_2$, and coal may be gasified by the $CO_2$; therefore, the combustion of coal in the $O_2/CO_2$ atmosphere is different from that in $O_2/N_2$ atmosphere.[11] The replacement of $N_2$ by $CO_2$ will decrease the speed of propagation and stability of the flame and gas temperature while increasing the unburned carbon content. The endothermic gasification reactions may tend also to cool the particles and reduce their oxidation rates. Therefore, higher $O_2$ concentrations are used in oxy-fuel combustion boilers to keep a similar adiabatic flame temperature and consequently similar heat transfer characteristics within the furnace.[11] It has also been reported that combustion in an $O_2/CO_2$ environment is delayed to a small extent compared with that in an $O_2/N_2$ environment at the same $O_2$ concentration.[12] Similar to pulverized coal combustion, coal gangue combustion also faces environmental concerns regarding the generation of greenhouse gases. In conventional coal combustion, $N_2$ from the air dilutes the $CO_2$ concentration and results in only about 15 vol % $CO_2$ concentration in the flue gas; therefore, the capture of $CO_2$ from flue gas is difficult.[13−16] Pure $O_2$ or a mixture of $O_2$ and recycled flue gas can be used to generate high concentration $CO_2$, which is ready for sequestration.[9] Recycled flue gas is used to control flame temperature.[12]

**Received:** January 23, 2013
**Revised:** May 7, 2013

   dx.doi.org/10.1021/ef400411w | *Energy Fuels* XXXX, XXX, XXX−XXX

**Table 1. Proximate and Ultimate Analyses of Coal Gangue[a]**

| proximate analysis (wt %) | | | | ultimate analysis (wt %, daf) | | | | | |
|---|---|---|---|---|---|---|---|---|---|
| M (ad) | A (ad) | VM (ad) | FC (ad) | C | H | O[b] | N | S | LHV (MJ/kg) |
| 3.64 | 68.38 | 14.73 | 13.25 | 20.43 | 1.75 | 6.41 | 0.31 | 0.13 | 8.32 |

[a]ad, air dried; daf, dry ash free. [b]By difference.

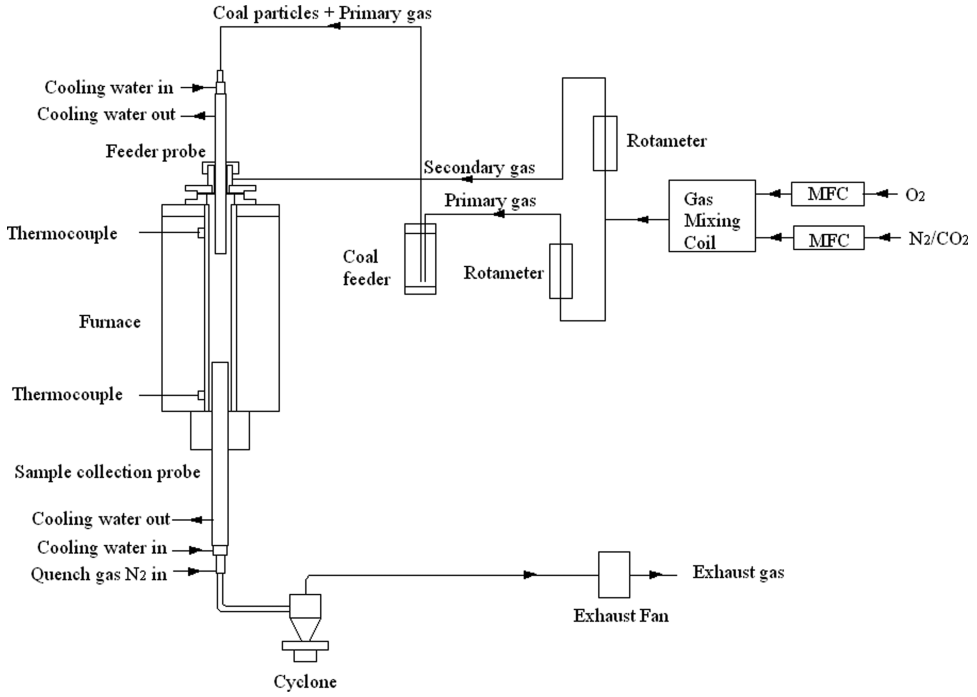


**Figure 1.** Schematic diagram of the DTF experimental setup.

Oxy-fuel combustion has been studied extensively for different types of coals but has received less attention for coal gangue. Coal gangue combustion faces some difficulties, such as high ash content, burn-out difficulty, and flame instability. Systematic study of coal gangue combustion is necessary in order to investigate these issues. However, very little has been reported in the literature on coal gangue combustion characteristics. In this paper, pyrolysis and combustion behavior of a low-rank coal gangue is investigated at different temperatures and under both air and oxy-fuel conditions with different $O_2$ concentrations by using a drop tube furnace (DTF) and thermogravimetric analysis (TGA). The mineral phase transformations were also investigated by means of XRD analysis.

## 2. EXPERIMENTAL SECTION

**2.1. Sample Preparation.** A Chinese low-rank coal gangue was used in the experiments, and its proximate and ultimate analyses are given in Table 1. The coal gangue samples were crushed and sieved into a 63−90 $\mu$m particle size cut.

**2.2. DTF Experiments.** The schematic of the drop tube furnace (DTF) experimental setup used for this study is shown in Figure 1. The experimental parameters of coal gangue combustion in DTF are given in Table 2. Pyrolysis and combustion experiments were conducted at 800, 1000, and 1200 °C, respectively. The furnace temperature was measured with two thermocouples that were installed in the upper and lower sections of the furnace (Figure 1). The coal gangue samples and primary gas mixture of 300 L/h ($N_2$, $CO_2$, $O_2/N_2$, or $O_2/CO_2$) were fed from the top of the furnace through a water-cooled feeder. The bottom of the feeder was inserted into the electrically heated furnace. A coal feeding rate of 5 g/h was used. The secondary gas of 200 L/h was preheated and introduced into the furnace through the annulus between the central tube and the Kao wool shield for the feeder. A water-cooled gas-quenched sampling probe was used to collect char from the bottom of the furnace. The residence time was about 0.4−0.6 s. The ash content of each char sample was measured, according to which the burnout of coal sample was calculated. In DTF experiments, each run was repeated three times, and the results presented in the following sections are the average of three measurements.

**Table 2. Experimental Parameters of Coal Gangue Combustion in Drop Tube Furnace**

| exptl parameter | condition |
|---|---|
| temp (°C) | 800, 1000, 1200 |
| gas composition | $CO_2$, $N_2$, $O_2/CO_2$, $O_2/N_2$ |
| primary gas flow (L/h) | 300 |
| secondary gas flow (L/h) | 200 |
| furnace inner diameter (m) | 0.09 |
| length of furnace heating zone (m) | 0.50 |
| inner diameter of the feeder (mm) | 2.26 |
| thermocouple type | platinum rhodium (S) |

Burnout during combustion was determined using an ash tracer method according to the following equation:[17,18]

$$\text{burnout} = 100\left[\frac{1 - (A_{coal} - A_{char})}{1 - A_{coal}}\right] \quad (1)$$

where $A_{coal}$ and $A_{char}$ are the ash content of the coal gangue and char, respectively. The difference between the actual volatile yield and that from the proximate volatile matter content may be reflected by the $R$ factor, which was defined as follows:[19]


dx.doi.org/10.1021/ef400411w | Energy Fuels XXXX, XXX, XXX−XXX

$$R \text{ factor} = \frac{\text{actual volatile yield } (V^*)}{\text{proximate volatile matter content (VM)}} \quad (2)$$

**2.3. Thermogravimetric Analysis (TGA).** A PerkinElmer Diamond TG/DTA 6300 was used for thermogravimetric combustion experiments. Experimental conditions have been constrained to permit direct comparison of different samples and to ensure repeatability of the experimental results. Preliminary experiments for examination of repeatability of the experimental results in one testing condition were conducted three times. In preliminary tests, combustion experiments were carried out using 5 mg coal gangue with 63−90 $\mu$m particle size under 21% $O_2$/79% $N_2$ condition. The results showed that the TG and DTG curves superposed perfectly and the error was acceptable, as shown in Figure 2. Pyrolysis experiments were carried out under $N_2$ and $CO_2$ atmospheres which were the diluting gases of air and oxy-fuel environments, respectively. The required combustion environments were formed by mixing two gases in the desired ratio by using two different mass flow controllers in order to regulate the flow rates of the gases. The $O_2$ concentrations used in this study were 21, 30, and 40 vol %, which were mixed with $N_2$ or $CO_2$ for a total flow rate of 100 mL/min. $N_2$ (30 mL/min) was used as instrument protective gas. In combustion experiments 5 ± 0.1 mg of coal gangue was heated from room temperature to a maximum temperature of 1000 °C with a 10 °C/min heating rate. The temperature of the sample was measured with a type S thermocouple with an accuracy of ±1.5 °C.

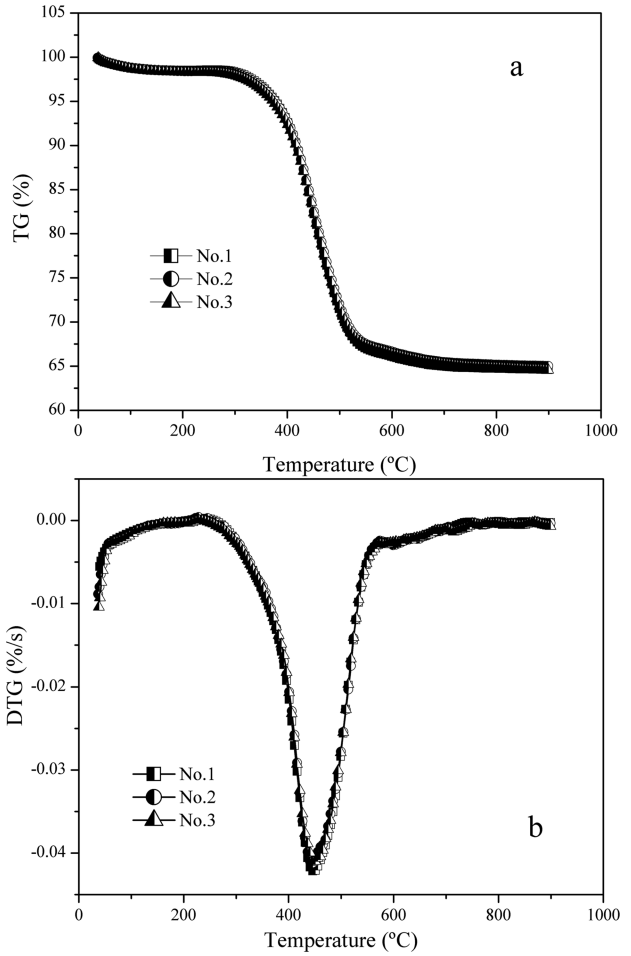


**Figure 2.** TG and DTG curves of preliminary tests.

The specific reactivity ($R_c$) of the char at any given time ($t$) was calculated from the following equation:[20−22]

$$R_c = -\frac{1}{w}\frac{dw}{dt} \quad (3)$$

where $w$ is the weight (dry, ash-free basis) of the char sample at any given time $t$.

**2.4. Determination of Combustion Characteristic Parameters.** There are several methods to determine the combustion characteristic temperatures.[13,23,24] The characteristic temperatures obtained from different methods are usually slightly different, but the values can be compared quantitatively as long as a consistent definition of these quantities is used.[23] TGA and DTG profiles obtained during pyrolysis and combustion experiments were used to determine characteristic parameters such as ignition temperature ($T_i$), burnout temperature ($T_b$), and peak temperature ($T_{max}$). Ignition temperature was defined as the temperature at which coal started burning. We adopted three different methods in determining the ignition temperature ($T_i$). In the first method (M1), the ignition temperature was defined as the temperature at which the combustion rate raised to 1 wt %/min at the start of a major combustion process.[23,25] In the second method (M2), $T_i$ was taken as the temperature at which the weight loss curves in the oxidation and pyrolysis experiments diverge.[12,26] The third method (M3) was the TG-DTG tangent method reported by Li et al.[13] As shown in Figure 3, in M3 the ignition temperature ($T_i$) was defined as the following: first, an extended TG initial level line was drawn; second, the position of point A on the TG curve was determined by making a vertical upward line passing through the peak of the DTG curve; third, the slope of the TG curve at point A was made to the TG curve at point A, which met the extended TG initial level line at point B; at last, one vertical line was made downward from point B, which intersected with the abscissa at point $T_i$. The corresponding temperature of this point was defined as the ignition temperature ($T_i$). The combustion profile of coal gangue under air combustion (5 mg of coal gangue with 63−90 $\mu$m particle size under 21% $O_2$/79% $N_2$ condition) was used in Figure 3 to demonstrate the TG-DTG tangent method.

The peak temperature $T_{max}$ was the temperature corresponding to the peak of the derivative thermogravimetric (DTG) curve.[23] The last characteristic temperature considered was the burnout temperature, which represented the temperature where sample oxidation was completed. It was taken as the point immediately before reaction ceased, when the rate of weight loss was 1 wt %/min.[12,27]

The values of ignition temperature ($T_i$) (measured by M1), burnout temperature ($T_b$), and peak temperature ($T_{max}$) for the preliminary combustion experiments under 21% $O_2$/79% $N_2$ condition are presented in Table 3. As can be seen, these values showed very good repeatability of the combustion experiments.

**2.5. Evaluation of Combustion Kinetics.** The differential method (utilizing the rate of weight loss) and integral method (utilizing weight loss vs temperature data directly) are the two main methods to determine the apparent activation energy and pre-exponential factor.[23,24,28−30] Several specific equations have been used for these two methods. These kinetic model functions have been developed on the basis of physical−geometrical assumptions.[31] It is reported in the literature that the trustworthy values of kinetics data of a solid state reaction could not be determined by a single TG curve, since the kinetic model functions are difficult to be discriminated in both of the above methods.[31−34] Furthermore, it has also been reported that any theoretical TG curve from a linear heating experiment fits most of the kinetics equations reported in the literature; however, the activation energies calculated by these equations vary considerably for a single experiment and it is impossible to select the most appropriate function obeyed by the reaction.[31] To overcome the above limitations, we have determined the values of $E_a$ by use of the isoconversional method.[35,36] This procedure includes the advantage of allowing the calculation of the activation energy without prior knowledge of the $g(\alpha)$ function. There have been many equations used for the isoconversional method, and we chose the equation of Flynn−Wall−Ozawa.[37−39]

According to the Arrhenius law,

$$\frac{d\alpha}{dt} = Ae^{-E_a/RT}f(\alpha) \quad (4)$$


dx.doi.org/10.1021/ef400411w | Energy Fuels XXXX, XXX, XXX−XXX

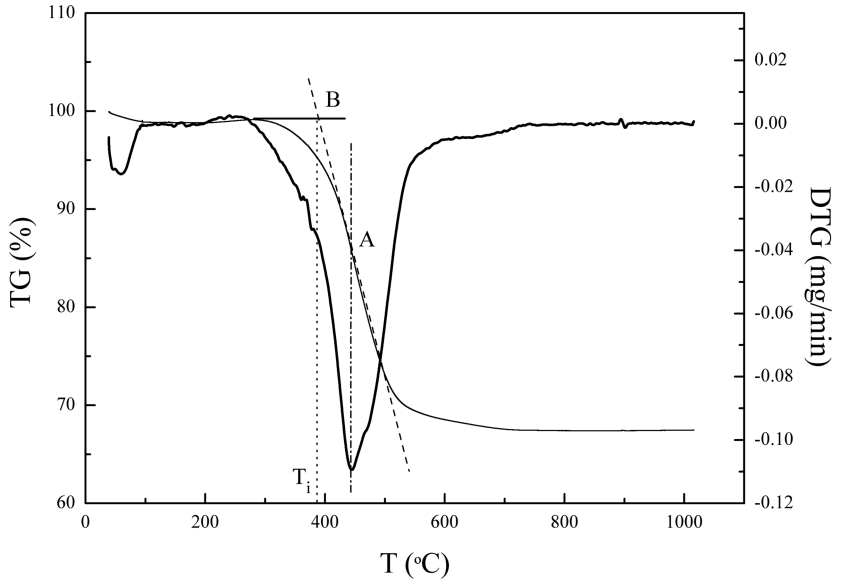


**Figure 3.** Determination of ignition temperature ($T_i$) with the tangent method.

**Table 3. Combustion Parameters of Coal Gangue in Preliminary Experiments**

| 21% $O_2$/79% $N_2$ | No. 1 | No. 2 | No. 3 |
|---|---|---|---|
| $T_i$ (°C) | 385 | 384 | 386 |
| $T_b$ (°C) | 517 | 519 | 517 |
| $T_{max}$ (°C) | 447 | 446 | 448 |

where $f(\alpha)$ is a function, the type of which depends on the reaction mechanism, $T$ is the sample temperature that was measured during TGA tests using a very thin thermocouple attached to the crucible from the bottom, $A$ is the pre-exponential factor, $E_a$ is the activation energy, $R$ is the universal gas constant, and $\alpha$ is the conversion fraction obtained from TG/DTG curves:

$$\alpha = \frac{m_0 - m_t}{m_0 - m_\infty} \tag{5}$$

where $m_0$ is the initial mass of coal gangue, $m_t$ is the mass of coal gangue at a time $t$, and $m_\infty$ is the final mass of coal gangue after the reaction. The integral form of the rate equation can be expressed as follows:

$$g(\alpha) = \frac{AE}{\beta R} p(\chi) \tag{6}$$

where $g(\alpha)$ is the integral function of $f(\alpha)$, $\beta = dT/dt$ represents the heating rate, $x = E/RT$, and the function $p(x)$ can be expressed as the following:

$$p(\chi) = \int_\chi^\infty \frac{\exp(-\chi)}{\chi^2}\, dx \tag{7}$$

Doyle[40] reported a linear relationship between log $p(x)$ and $x$:

$$\log p(\chi) = -2.315 - 0.4567\chi \tag{8}$$

Combining eqs 6 and 8:

$$\log g(\alpha) = \log \frac{AE}{\beta R} - 2.315 - 0.4567\frac{E}{RT} \tag{9}$$

For a number of experiments with different heating rates, the Flynn–Wall–Ozawa equation for the same conversion rate can be written as follows:

$$\log \beta = C - 0.4567\frac{E}{RT} \tag{10}$$

where $C$ is a constant. The values of $E_a$ could be calculated from the slope of a plot of log $\beta$ versus the reciprocal of temperature.

**2.6. Mineral Matter Analysis.** The mineral phase transformation was analyzed by X-ray diffraction techniques (XRD) using a Shimadzu XRD-7000 X-ray diffractometer. The X-ray pattern of pulverized coal gangue was recorded with a step-scanning method in the range of $2\theta$ = 10–90°. The minerals in each sample were accounted from the diffractograms by reference to the ICDD powder diffraction database.

## 3. RESULTS AND DISCUSSION

**3.1. Pyrolysis Characteristics of Coal Gangue in $CO_2$ and $N_2$ Atmospheres.** Coal pyrolysis can be described as the thermal decomposition of the organic components in an oxygen-free atmosphere to yield char, oil, and gaseous products, which in TGA study generally includes two parts of moisture release and devolatilization. Figure 4 shows the pyrolysis characteristics of coal gangue in $CO_2$ and $N_2$ atmospheres, which are the main diluting gases of oxy-fuel and air environment, respectively. It can be seen that the two DTG curves showed a similar trend up to around 200 °C which corresponded to moisture release from coal gangue. As can be seen in Figure 4b, coal gangue pyrolysis in $N_2$ environment had two stages of moisture release (up to 200 °C) and devolatilization (in the range of 200–800 °C) but coal pyrolysis in $CO_2$ atmosphere also had a third stage of char gasification by $CO_2$ in a higher temperature zone (>800 °C). The pyrolysis peak rate occurred at about 450 and 476 °C in $N_2$ and $CO_2$ atmospheres, respectively, which showed a delay in devolatilization under $CO_2$ conditions (Figure 4b). Similar results have been reported by Wall et al.[9] In the temperature range of 200–800 °C, the mass loss rate of coal gangue under $N_2$ was higher than that under $CO_2$. This was due to the difference in properties of the bulk gases. $CO_2$ has higher specific heat than $N_2$, which results in higher surface temperature of coal particles under $N_2$ than that under $CO_2$ as reported by Zhang et al.[41] and Arias et al.[42] Above 800 °C, the mass loss rate of coal gangue in $CO_2$ atmosphere was higher than that in $N_2$ atmosphere, which was attributed to the char gasification by $CO_2$.[13] Wang et al.[23] also reported the char–$CO_2$ gasification reaction at around 810 °C. The initiation of a char gasification reaction at around 700 °C for Turkish lignite


dx.doi.org/10.1021/ef400411w | Energy Fuels XXXX, XXX, XXX–XXX

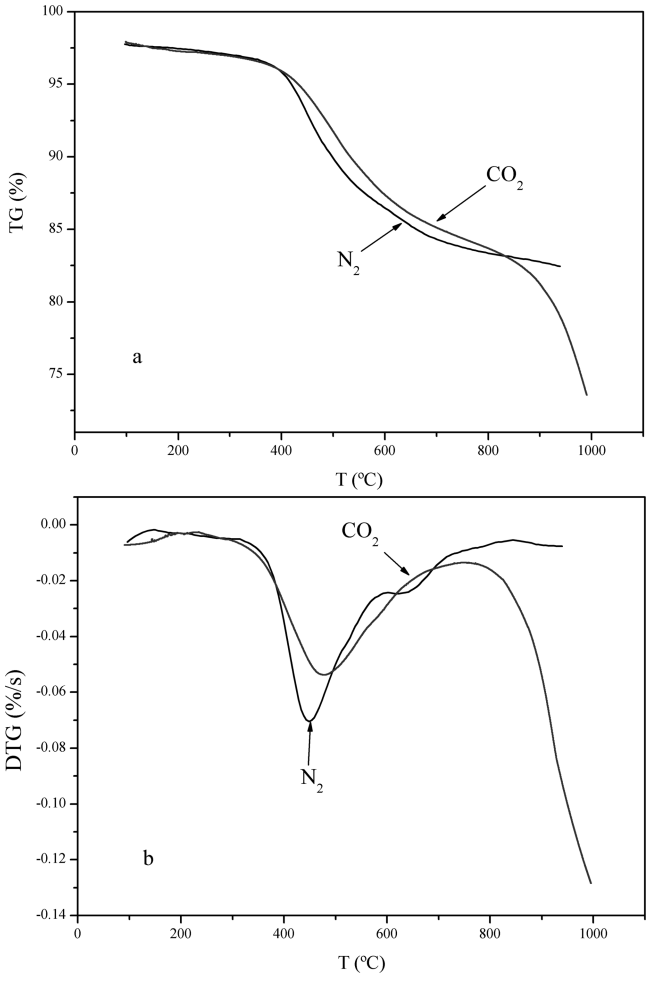


**Figure 4.** Pyrolysis of coal gangue in $N_2$ and $CO_2$ atmospheres in TGA, indicating an increased reactivity in $CO_2$ at temperatures above 800 °C: (a) TG curves; (b) DTG curves.

has also been reported.[12] Hence, the char−$CO_2$ gasification reaction of coal gangue may play an important role when the temperature is above 800 °C in oxy-fuel combustion. There is a difference among the critical temperatures of the char−$CO_2$ reaction for coal and coal gangue due to the high ash content of coal gangue.

**3.2. Yields of Volatile Matter and Burnout in DTF.** The pyrolysis of coal gangue in DTF was carried out to investigate the gasification effect of $CO_2$ on coal gangue. The apparent volatile yields of coal gangue studied in $N_2$ and $CO_2$ at low temperature (800 °C) and high temperature (1200 °C) in the drop tube furnace are shown in Table 4. The volatile yield of coal gangue increased when the pyrolysis temperature increased. At high temperatures, the actual volatile yield ($V^*$) was higher than the respective volatile yield obtained by proximate analysis (VM). The actual volatile yield and, therefore, the $R$ factor were higher in $CO_2$ than $N_2$ at higher temperatures, since the gasification reaction by $CO_2$ took place. TG and DTG curves of coal gangue pyrolysis in $N_2$ and $CO_2$ atmospheres (Figure 4) explain the greater mass loss in $CO_2$. It can be clearly seen that the weight loss rate increased significantly in $CO_2$ at around 800 °C. The increase in volatile matter yield at higher temperatures was attributed to the commencement of the char−$CO_2$ gasification reaction.[22,43]

Figure 5 shows the burnout of coal gangue at different $O_2$ concentrations and combustion temperatures in $CO_2$ and $N_2$ atmospheres. The burnout value obtained under the 21% $O_2$/79% $CO_2$ atmosphere was slightly lower than that reached under 21% $O_2$/79% $N_2$ conditions. The specific heat capacity of the diluent gas was an important factor affecting char surface temperature for any concentration of $O_2$.[41] Higher specific molar heat of $CO_2$ resulted in higher heating capacity of the surrounding gases, which leads to lower flame and gas temperatures under this atmosphere, as reported by Zhang et al.[41] and Arias et al.[42] As a result, the combustion rate of the char and the fuel burnout values decreased under the 21% $O_2$/79% $CO_2$ condition. Lower burnout values under 21% $O_2$/79% $CO_2$ than that under the 21% $O_2$/79% $N_2$ condition were also attributed to lower diffusivity of $O_2$ in $CO_2$ than in $N_2$, which impeded the $O_2$ transport to the particle surface, reducing the combustion rate of the volatile matter and char.[17] Zhang et al.[41] suggested that, in $CO_2$ atmosphere, the CO gas formed as a result of the $CO_2$-char gasification reaction mixed with tarry species to form a large volatile cloud around the particle. Instead of single particle ignition, cloud was ignited in $O_2$/$CO_2$ when the volatiles were accumulated to a critical concentration. To achieve similar coal ignition intensity within air, higher $O_2$ fractions than air-firing become necessary in oxy-fuel combustion.[41,44]

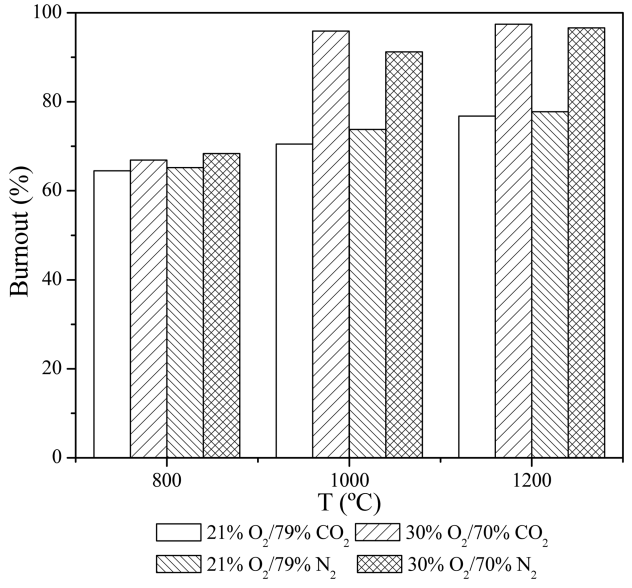


**Figure 5.** Comparison of the burnout of coal gangue at different $O_2$ partial pressures in $CO_2$ and $N_2$ atmospheres in DTF at different temperatures.

**Table 4. Pyrolysis of Coal Gangue in $N_2$ and $CO_2$ Atmospheres in Drop Tube Furnace Experiments at 800 and 1200 °C**

| pyrolysis temp (°C) | VM (wt % daf) | $V^*$ ($N_2$) | $R$ factor ($N_2$) | $V^*$ ($CO_2$) | $R$ factor ($CO_2$) |
|---|---|---|---|---|---|
| 800 | 52.66 | 64.14 | 1.218 | 52.01 | 0.987 |
| 1200 | 52.66 | 90.50 | 1.718 | 92.26 | 1.752 |

As can be seen in Figure 5, the increase in $O_2$ concentration led to an increase in the coal gangue burnout under all conditions. At 800 °C, increasing $O_2$ concentration from 21 to 30 vol % resulted in the increase of coal gangue burnout under air and oxy-fuel conditions by 3.16% and 2.41%, respectively.


dx.doi.org/10.1021/ef400411w | Energy Fuels XXXX, XXX, XXX−XXX

During combustion at 1000 °C, with a similar increase in $O_2$ concentration, the burnout increased by 17.4% and 25.43% in air and oxy-fuel combustion, respectively. At 1200 °C, the increase in burnout was 18.85% and 20.64% under air and oxy-fuel combustion, respectively, when $O_2$ concentration was increased from 21 to 30 vol %. The higher oxygen concentration caused an increase in the char combustion rate, together with a decrease in the ignition temperature. Similar results were reported by Liu et al. for a bituminous coal.[44] The increase in the mass flux rate of $O_2$ to the particle surface at higher $O_2$ concentrations promoted the consumption rate of the volatiles.[45] This provided extra heat feedback to the particle, enhancing devolatilization, ignition, and combustion.[11] Coal gangue burnout increased significantly when temperature was increased from 800 to 1000 °C. However, further increasing temperature to 1200 °C did not have a significant effect on burnout, especially at higher $O_2$ concentrations. There was a 2.4% difference between the burnout at 21% $O_2$/79% $CO_2$ and 30% $O_2$/70% $CO_2$ at 800 °C, but this difference increased significantly to 20.64% after combustion at 1000 °C, indicating that higher oxygen concentrations are favorable in oxy-fuel combustion at higher temperatures. Very high burnouts of 95.92% and 97.41% were achieved under 30% $O_2$/70% $CO_2$ conditions at 1000 and 1200 °C, respectively.

**3.3. Combustion Characteristics of Coal Gangue under $N_2/O_2$ and $CO_2$/O2 Conditions in TGA.** The TG and DTG curves of coal gangue under $O_2/CO_2$ and $O_2/N_2$ conditions are shown in Figures 6 and 7, respectively. It can be seen that, with the increase of $O_2$ concentration, the mass loss rate increased, TG and DTG curves of coal gangue combustion shifted to a lower temperature zone under both $O_2/CO_2$ and $O_2/N_2$ conditions, and complete combustion was achieved at lower temperatures and shorter times. Similar results have been reported by Li et al.[13] The combustion characteristics of coal gangue organic matter were enhanced due to the presence of high $O_2$ concentration.[13,22,43] This can be attributed to a higher amount of $O_2$ adsorption on the particle surface at higher $O_2$ concentrations.

The combustion characteristic parameters determined from the burning profiles in Figures 6 and 7 are summarized in Table 5. From combustion profiles (Figures 6 and 7) and Table 5, it can be seen that, with the $O_2$ concentration increase, the temperature corresponding to the maximum mass loss of sample ($T_{max}$) decreased, and the peak value of the DTG curve increased, showing higher maximum weight loss at lower temperature. As can be seen in Table 5, the ignition temperature ($T_i$) and burnout temperature ($T_b$) decreased at higher $O_2$ concentrations for all combustion conditions, showing the improved combustion performance at higher $O_2$ partial pressures. The ignition temperature in Table 5 was calculated using the three methods described in section 2.4. The changes in $T_i$ calculated from M1, M2, and M3 followed a similar trend. The values of $T_i$ obtained from these methods were in the following order: M1 > M3 > M2. Using M1, M2, and M3 methods, when $O_2$ concentration increased from 21 to 40 vol %, the $T_i$ under oxy-fuel combustion decreased by 14, 24, and 15 °C, respectively. The decrease in $T_i$ values was 8, 16, and 10 °C in an $N_2$ environment. When $O_2$ partial pressure increased from 21 to 40 vol %, the $T_b$ decreased by 35 and 13 °C in $CO_2$ and $N_2$ conditions, respectively. Similar results have been reported by Arias et al.[42] and Wang et al.[23]

Comparison of the combustion characteristic parameters in $N_2/O_2$ and $CO_2/O_2$ environments (Table 5) revealed that the

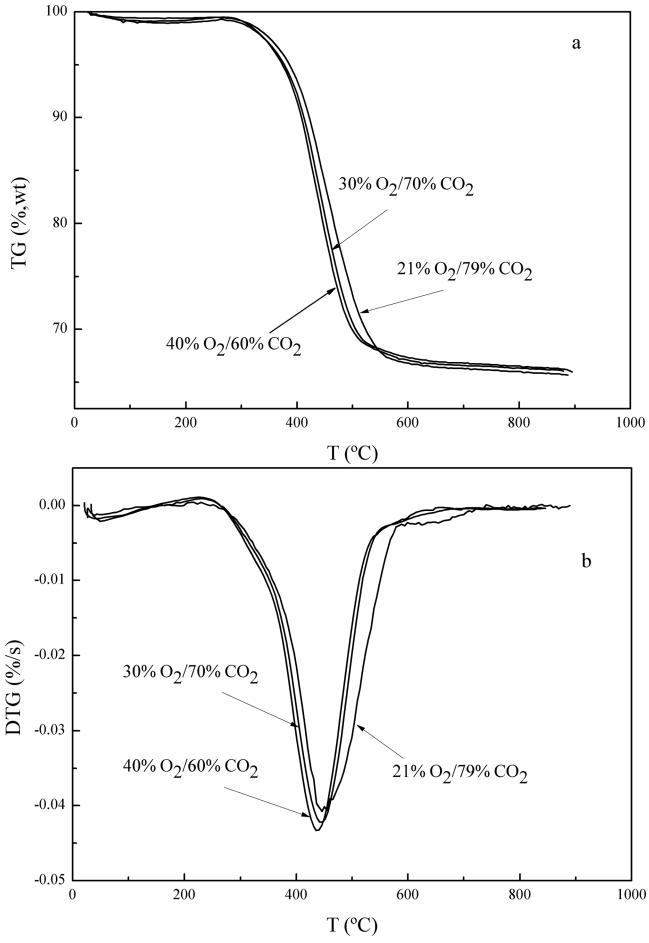


**Figure 6.** TG and DTG curves of coal gangue combustion in $O_2/CO_2$ environments and at different $O_2$ concentrations: (a) TG curves; (b) DTG curves.

combustion performance in the $N_2/O_2$ environment was better than that in the $CO_2/O_2$ environment at 21 vol % $O_2$ concentration. This can be attributed to the different diffusivity of $O_2$ in $N_2$ and $CO_2$. The $O_2$ diffusion rate in $CO_2$ is 0.8 times that in $N_2$.[9] The lower diffusivity of $O_2$ in $CO_2$ compared to that in $N_2$ affects the transport of $O_2$ to the surface of the particles, leading to the reduced combustion rates. Combustion of released volatile matter is also affected by lower $O_2$ diffusivity in $CO_2$. Replacing $N_2$ by $CO_2$ was favorable to the burnout of coal gangue at higher $O_2$ concentrations. This conclusion can be confirmed by values of ignition temperature ($T_i$) and burnout temperature ($T_b$) in both $N_2$ and $CO_2$ environment in Table 5. The ignition temperature ($T_i$) values in $CO_2$ were higher than those in $N_2$ atmosphere at 21 vol % $O_2$ concentrations. However, the $T_i$ was lower in $CO_2$ than that in $N_2$ at 30 and 40 vol % $O_2$ partial pressures. Similar results were reported by Riaza et al.[11]

Moreover, the coal reactivity index ($R_C$) was used to evaluate the burning performance of pulverized coal gangue:[46]

$$R_C = \frac{1}{W_0}\left(\frac{dw}{dt}\right)_{max} \quad (11)$$

where $(dw/dt)_{max}$ is the maximum combustion rate and $w_0$ is the initial weight of sample. The greater the $R_C$ value, the higher combustion reactivity is. As can be seen in Figure 8, the coal gangue reactivity was higher in $N_2$ than that in $CO_2$ atmosphere


dx.doi.org/10.1021/ef400411w | Energy Fuels XXXX, XXX, XXX−XXX

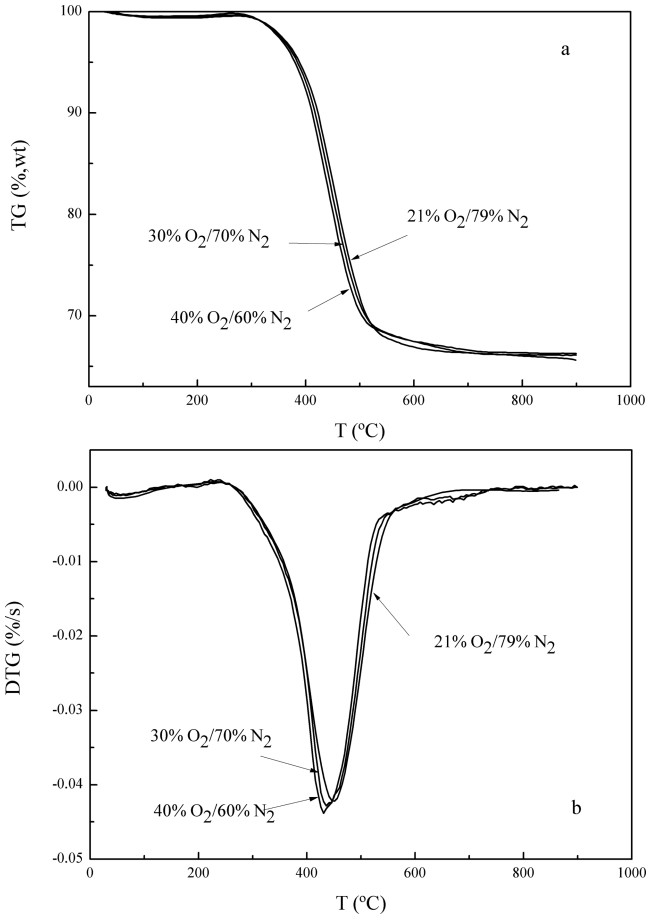


**Figure 7.** TG and DTG curves of coal gangue combustion in $O_2/N_2$ environments and at different $O_2$ concentrations: (a) TG curves; (b) DTG curves.

**Table 5. Combustion Characteristics of Coal Gangue in Different Gas Environments in a Drop Tube Furnace**

| gas composition (vol %) | | | $T_i$ (°C) | | | | | |
|---|---|---|---|---|---|---|---|---|
| $O_2$ | $N_2$ | $CO_2$ | M1 | M2 | M3 | $T_b$ (°C) | $T_{max}$ (°C) | $DTG_{max}$ (wt %/min) |
| 21 | 79 | | 383 | 376 | 380 | 514 | 444 | 2.52 |
| 30 | 70 | | 381 | 370 | 371 | 508 | 433 | 2.56 |
| 40 | 60 | | 375 | 360 | 370 | 501 | 431 | 2.63 |
| 21 | | 79 | 387 | 381 | 382 | 532 | 447 | 2.42 |
| 30 | | 70 | 378 | 365 | 370 | 505 | 443 | 2.53 |
| 40 | | 60 | 373 | 357 | 367 | 497 | 437 | 2.60 |

at 21 vol % and 30 vol % $O_2$ concentration. Prior to ignition, the coal gangue particles are heated in ambient environment to combustion temperature. The radiant heat from the particles then increases the surrounding gas temperature. Due to the higher specific molar heat of $CO_2$, more heat is needed to increase the temperature under oxy-fuel conditions.[11] This results in a lower gas temperature and, therefore, a reduction in the particle temperature during oxy-fuel combustion in comparison to combustion in air at low $O_2$ concentration.[47] When $O_2$ concentration increased to 30 vol %, the difference between the coal gangue reactivity under air and oxy-fuel conditions decreased significantly, and finally, coal gangue showed higher reactivity in $CO_2$ than in $N_2$ at 40 vol % $O_2$ concentration.[47] This can be attributed to the increase in the

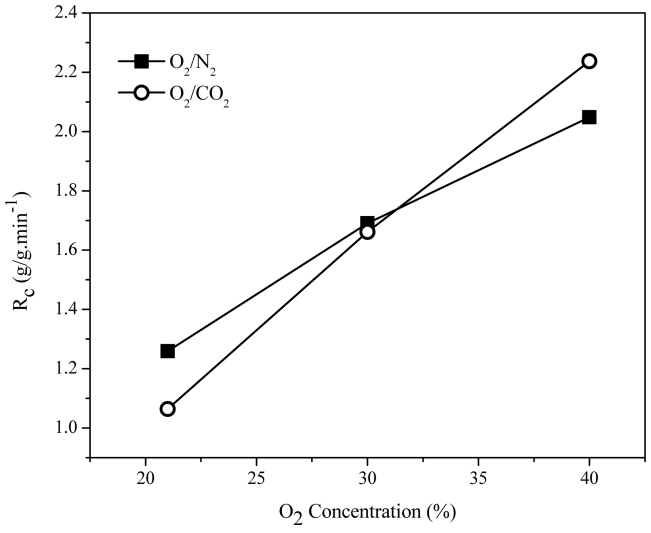


**Figure 8.** Coal gangue combustion reactivity ($R_C$) in different gas environments.

mass flux rate of $O_2$ to the fuel surface, the rate of devolatilization, and the oxidation rate of the volatiles, which resulted in shorter coal gangue particle ignition time.[41] With $O_2$ concentrations increase, CO oxidation in the boundary layers of char particles and the gasification of the char by $CO_2$ becomes significant and pulverized coal char particles burn under increasing kinetic control.[13,48]

**3.4. Combustion Kinetics.** For calculating the $E_a$ values, coal gangue combustion tests on TGA were carried out at four different heating rates (5, 10, 12, and 15 °C/min) from 30 to 1000 °C under different atmospheres. The combustion profiles are shown in Figure 9. As can be seen, with increasing the

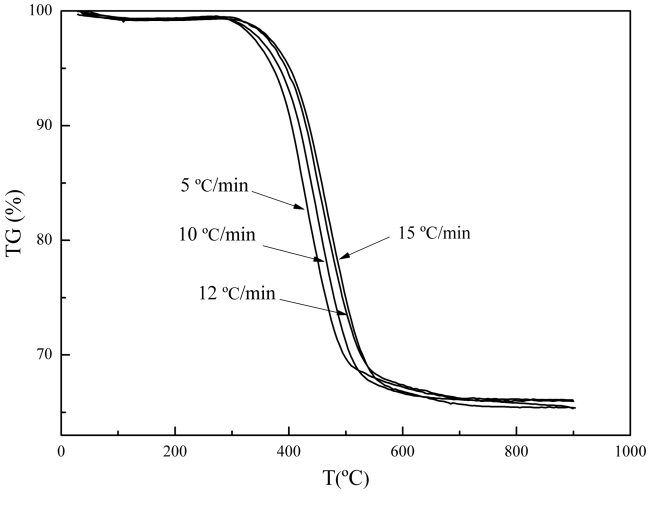


**Figure 9.** Effect of heating rate on coal gangue combustion profiles in 21% $O_2$/79% $N_2$.

heating rate, TG curves shifted to a higher temperature zone; however, the combustion mechanism did not seem to change. The values of $E_a$ as a function of $\alpha$ under air and $CO_2$ at different $O_2$ concentrations are shown in Figure 10. The result indicated that the $E_a$ variation trend was similar under all combustion conditions. At the beginning of the combustion process, the lower activation energy values were due to the active volatile matter present in the coal gangue and then the


dx.doi.org/10.1021/ef400411w | Energy Fuels XXXX, XXX, XXX−XXX

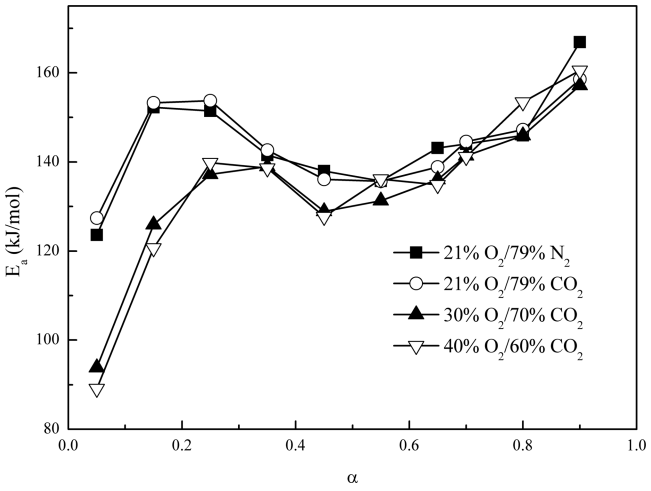


**Figure 10.** Activation energy of coal gangue during combustion under different conditions.

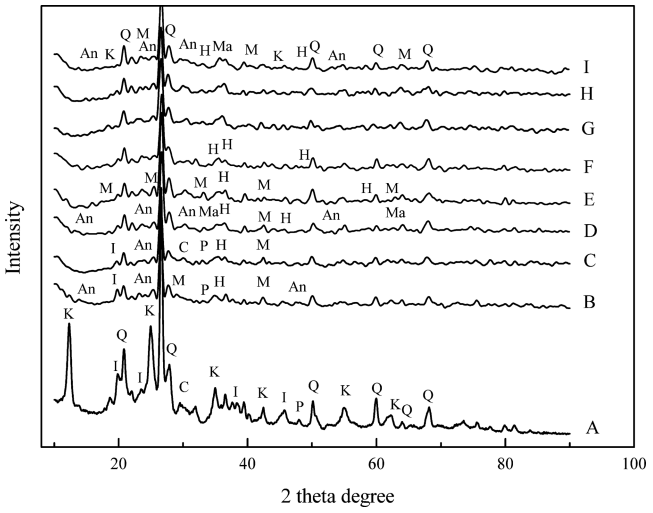


**Figure 11.** X-ray diffraction patterns of chars of coal gangue after combustion at different temperatures. The mineral phases identified are as follows: K-kaolinlte, I-illite, Q-quartz, C-calcite, P-pyrite, H-hematite, An-anhydrite, Ma-magnetite, M-mullite. Combustion conditions: (A) raw coal gangue; (B) 800 °C, 21% $O_2$/79% $N_2$; (C) 800 °C, 21% $O_2$/79% $CO_2$; (D) 1000 °C, 21% $O_2$/79% $N_2$; (E) 1000 °C, 21% $O_2$/79% $CO_2$; (F) 1000 °C, 30% $O_2$/70% $CO_2$; (G) 1200 °C, 21% $O_2$/79% $N_2$; (H) 1200 °C, 21% $O_2$/79% $CO_2$; (I) 1200 °C, 30% $O_2$/70% $CO_2$.

activation energy values increased, which was attributed to the decrease of volatile matter and high concentration of fixed carbon present in the coal gangue. Activation energy values decreased at around 50% conversion, possibly due to the intense combustion of carbon. Finally, with the decrease in carbon content and increase in ash content, the $E_a$ values increased until the complete conversion was achieved. The value of $\alpha$ in the range 0.05−0.5 corresponded to the temperature range of about 300−470 °C, which was the main zone of combustion. In this zone, the activation energy values of coal gangue combustion in $CO_2$ were slightly higher than that in $N_2$ at 21 vol % $O_2$ concentration (Figure 10). However, increasing $O_2$ partial pressure significantly decreased the activation energy for combustion in $CO_2$ to lower values than that in air, indicating that increasing $O_2$ concentration in $CO_2$ improved the combustion characteristics for coal gangue. To achieve similar combustion characteristics in air, 21−30% oxygen was required in oxy-fuel combustion of coal gangue.

**3.5. Mineral Transformation.** Due to the high ash content, the inorganic matter in coal gangue may have significant effects on its morphological changes during combustion. Therefore, the mineral matter reactions during combustion were investigated by the XRD technique. The possible mineral reactions during coal gangue combustion as a function of temperature and combustion environment were analyzed by XRD, and the results are shown in Figure 11. In raw coal gangue, the mineral phases were kaolinite, quartz, illite, pyrite, and calcite. Pyrite was still present as coal gangue ash at 800 °C, but its peak intensities disappeared after combustion at 1000 °C.[49,50] Hematite and magnetite were formed at 800 and 1000 °C, respectively. Hatt and Bull[51] suggested that hematite formation can be promoted with rapid quenching of iron in the air while exposure of iron to hot flue gas for extended periods of time promotes the formation of magnetite.

With increasing combustion temperature, the peak intensities of hematite and magnetite increased. It was also observed that, at 1000 °C, hematite was formed more in 30% $O_2$/70% $CO_2$ than 21% $O_2$/79% $CO_2$, possibly due to higher oxygen partial pressure. The peak intensities of kaolinite decreased continuously with increasing temperature due to phase transformation from kaolinite to metakaolinite.[52] The appearance of new diffraction peaks for combusted coal gangue demonstrated the generation of new substances, such as hematite, lime, and anhydrite.[49] Mullite was formed as a result of decomposition of clay minerals. Mullite normally forms through solid-state reactions primarily from kaolinite, and to a lesser extent from high-Al illite and illite/smectite.[49] Cristobalite was also reported to form from kaolinite heated to 900−1300 °C.[53] However, it seemed that the amount of cristabolite that might have formed in the combustion ashes of coal gangue was less than the detection limit of the XRD technique.

Calcite was present in coal gangue ash after combustion in 21% $O_2$/79% $CO_2$ at 800 °C but decomposed to lime at higher temperatures. Lime from decomposition of calcite reacted with $SO_2$ and $CO_2$ to form anhydrite at temperatures above 800 °C.[49,50] With raising the temperature, peak intensities of mullite and anhydrite increased continuously. The peak intensities of illite decreased after combustion at 800 °C under both air and oxy-fuel combustion and disappeared completely at higher temperatures. Quartz was present in all conditions; however, its peak intensities decreased after combustion due to partial melting, glass formation, and reaction with highly active $Al_2O_3$. Conversion of quartz to glass as a result of combustion at 1200−1300 °C has been reported by Mitchell and Gluskoter.[53] At 1200 °C, the minerals formed were similar regardless of combustion environment. The mineral phases were kaolinite, quartz, mullite, magnetite, hematite, and anhydrite at combustion temperatures of 1200 °C. The details of these conversion reactions were as follows:[6,49]

$$\text{pyrite } (FeS_2) + O_2 \xrightarrow{>800\,^\circ C} \text{hematite } (Fe_2O_3) + \text{magnetite } (Fe_3O_4) + SO_2 \quad (12)$$

$$\text{calcite } (CaCO_3) \xrightarrow{>800\,^\circ C} \text{lime } (CaO) + CO_2 \quad (13)$$

$$CaO + SO_2 + O_2 \xrightarrow{>800\,^\circ C} \text{anhydrite } (CaSO_4) \quad (14)$$


dx.doi.org/10.1021/ef400411w | Energy Fuels XXXX, XXX, XXX−XXX

$$\text{clay minerals} \xrightarrow{<600\,^{\circ}\text{C}} \text{dehydration and dehydroxylation} \xrightarrow{800-1000\,^{\circ}\text{C}} \text{glass} \xrightarrow{>1000\,^{\circ}\text{C}} \text{glass} + \text{mullite}\ (3(Al_2O_3)\cdot 2(SiO_2)) + \text{cristobalite}\ (SiO_2)$$

$$\text{quartz} \xrightarrow{>1100\,^{\circ}\text{C}} \text{partial melting and glass formation} \quad (15)$$

## 4. CONCLUSIONS

(1) The behavior of coal gangue during pyrolysis in $CO_2$ environments was different from that in $N_2$ due to the difference in bulk gas properties. At temperatures higher than 800 °C, the mass loss of coal gangue in $CO_2$ was higher than that in $N_2$ due to $CO_2$−char gasification.

(2) During DTF experiments, the increase in the $O_2$ partial pressure and combustion temperature led to an increase in the coal gangue burnout under all combustion conditions. The ignition of coal gangue in a $CO_2/O_2$ environment was delayed compared with that in a $N_2/O_2$ environment.

(3) In TGA studies, as the $O_2$ concentration increased, DTG profiles shifted to a lower temperature zone, burnout time shortened, and the peak value of the DTG curve increased, indicating a higher rate of weight loss at lower temperatures.

(4) Kinetic analysis of coal gangue samples was done using the isoconventional method. The $E_a$ variation trend was similar under all combustion conditions. The activation energy ($E_a$) in oxy-fuel combustion decreased with increasing $O_2$ concentration compared to that in air combustion.

(5) The mineral phases of raw coal gangue were kaolinite, quartz, illite, pyrite, and calcite. Pyrite was converted to hematite and magnetite at temperatures higher than 800 °C. Above 800 °C, calcite was decomposed to lime, which itself reacted with $SO_2$ to form anhydrite. Clay minerals formed mullite and quartz (glass) after combustion at 1000 °C. Quartz was partially melted and formed glass above 1100 °C. The mineral phases of ash were kaolinite, quartz, mullite, magnetite, hematite, and anhydrite after combustion at 1200 °C.

## AUTHOR INFORMATION

### Corresponding Author

*Tel: +86 412 5929105, Fax: +86 412 5929627, E-mail: jianglongyu@163.com.

### Notes

The authors declare no competing financial interest.

## ACKNOWLEDGMENTS

This study was supported by the Natural Science Foundation of China (21176109 and 21210102058). The authors gratefully acknowledge the financial support of the Australia−China Joint Coordination Group on Clean Coal Technology Research & Development Grants of Australian Government. We also acknowledge the funding support by Liaoning Talents Funding Program (LR201032) and Liaoning Outstanding Professorship Funding Program (2011) of Liaoning Province.

## REFERENCES

(1) Haibin, L.; Zhenling, L. Recycling utilization patterns of coal mining waste in China. *Resour., Conserv. Recycl.* **2010**, *54*, 1331−1340.

(2) Querol, X.; Izquierdo, M.; Monfort, E.; Alvarez, E.; Font, O.; Moreno, T.; Alastuey, A.; Zhuang, X.; Lu, W.; Wang, Y. Environmental characterization of burnt coal gangue banks at Yangquan, Shanxi Province, China. *Int. J. Coal Geol.* **2008**, *75*, 93−104.

(3) Zhou, B.; Shao, M. a.; Wen, M.; Wang, Q.; Horton, R. Effects of coal gangue content on water movement and solute transport in a China Loess Plateau soil. *CLEAN—Soil, Air, Water* **2010**, *38*, 1031−1038.

(4) Bell, F. G.; Stacey, T. R.; Genske, D. D. Mining subsidence and its effect on the environment: some differing examples. *Environ. Geol.* **2000**, *40*, 135−152.

(5) Chugh, Y. P.; Patwardhan, A. Mine-mouth power and process steam generation using fine coal waste fuel. *Resour., Conserv. Recycl.* **2004**, *40*, 225−243.

(6) Zhou, C.; Liu, G.; Yan, Z.; Fang, T.; Wang, R. Transformation behavior of mineral composition and trace elements during coal gangue combustion. *Fuel* **2012**, *97*, 644−650.

(7) Li, D.; Song, X.; Gong, C.; Pan, Z. Research on cementitious behavior and mechanism of pozzolanic cement with coal gangue. *Cem. Concr. Res.* **2006**, *36*, 1752−1759.

(8) Zhang, N.; Sun, H.; Liu, X.; Zhang, J. Early-age characteristics of red mud−coal gangue cementitious material. *J. Hazard. Mater.* **2009**, *167*, 927−932.

(9) Wall, T.; Liu, Y.; Spero, C.; Elliott, L.; Khare, S.; Rathnam, R.; Zeenathal, F.; Moghtaderi, B.; Buhre, B.; Sheng, C.; Gupta, R.; Yamada, T.; Makino, K.; Yu, J. An overview on oxyfuel coal combustion—state of the art research and technology development. *Chem. Eng. Res. Des.* **2009**, *87*, 1003−1016.

(10) Chen, L.; Yong, S. Z.; Ghoniem, A. F. Oxy-fuel combustion of pulverized coal: Characterization, fundamentals, stabilization and CFD modeling. *Prog. Energy Combust. Sci.* **2012**, *38*, 156−214.

(11) Riaza, J.; Gil, M. V.; Álvarez, L.; Pevida, C.; Pis, J. J.; Rubiera, F. Oxy-fuel combustion of coal and biomass blends. *Energy* **2012**, *41*, 429−435.

(12) Yuzbasi, N. S.; Selçuk, N. Air and oxy-fuel combustion characteristics of biomass/lignite blends in TGA-FTIR. *Fuel Process. Technol.* **2011**, *92*, 1101−1108.

(13) Li, Q.; Zhao, C.; Chen, X.; Wu, W.; Li, Y. Comparison of pulverized coal combustion in air and in $O_2/CO_2$ mixtures by thermogravimetric analysis. *J. Anal. Appl. Pyrolysis* **2009**, *85*, 521−528.

(14) Chakma, A. Separation of $CO_2$ and $SO_2$ from flue gas streams by liquid membranes. *Energy Convers. Manage.* **1995**, *36*, 405−410.

(15) Zhou, W.; Moyeda, D. Process evaluation of oxy-fuel combustion with flue gas recycle in a conventional utility boiler. *Energy Fuels* **2010**, *24*, 2162−2169.

(16) Wang, C.; Lei, M.; Yan, W.; Wang, S.; Jia, L. Combustion characteristics and ash formation of pulverized coal under pressurized oxy-fuel conditions. *Energy Fuels* **2011**, *25*, 4333−4344.

(17) Li, X.; Rathnam, R. K.; Yu, J.; Wang, Q.; Wall, T.; Meesri, C. Pyrolysis and combustion characteristics of an Indonesian low-rank coal under $O_2/N_2$ and $O_2/CO_2$ conditions. *Energy Fuels* **2010**, *24*, 160−164.

(18) Biswas, S.; Choudhury, N.; Sarkar, P.; Mukherjee, A.; Sahu, S. G.; Boral, P.; Choudhury, A. Studies on the combustion behaviour of blends of Indian coals by TGA and Drop Tube Furnace. *Fuel Process. Technol.* **2006**, *87*, 191−199.

(19) Kimber, G. M.; Gray, M. D. Rapid devolatilization of small coal particles. *Combust. Flame* **1967**, *11*, 360−362.

(20) Wu, H.; Hayashi, J.-i.; Chiba, T.; Takarada, T.; Li, C.-Z. Volatilisation and catalytic effects of alkali and alkaline earth metallic species during the pyrolysis and gasification of Victorian brown coal. Part V. Combined effects of Na concentration and char structure on char reactivity. *Fuel* **2004**, *83*, 23−30.

(21) Benfell, K. E.; Liu, G.-S.; Roberts, D. G.; Harris, D. J.; Lucas, J. A.; Bailey, J. G.; Wall, T. F. Modeling char combustion: The influence of parent coal petrography and pyrolysis pressure on the structure and

intrinsic reactivity of its char. *Proc. Combust. Inst.* **2000**, *28*, 2233−2241.
(22) Rathnam, R. K.; Elliott, L. K.; Wall, T. F.; Liu, Y.; Moghtaderi, B. Differences in reactivity of pulverised coal in air ($O_2/N_2$) and oxy-fuel ($O_2/CO_2$) conditions. *Fuel Process. Technol.* **2009**, *90*, 797−802.
(23) Wang, C. a.; Zhang, X.; Liu, Y.; Che, D. Pyrolysis and combustion characteristics of coals in oxyfuel combustion. *Appl. Energy* **2012**, *97*, 264−273.
(24) Yorulmaz, S. Y.; Atimtay, A. T. Investigation of combustion kinetics of treated and untreated waste wood samples with thermogravimetric analysis. *Fuel Process. Technol.* **2009**, *90*, 939−946.
(25) Wang, C. a.; Liu, Y.; Zhang, X.; Che, D. A study on coal properties and combustion characteristics of blended coals in northwestern China. *Energy Fuels* **2011**, *25*, 3634−3645.
(26) Jia, L.; Anthony, E. J.; Lau, I.; Wang, J. Study of coal and coke ignition in fluidized beds. *Fuel* **2006**, *85*, 635−642.
(27) Morgan, P. A.; Robertson, S. D.; Unsworth, J. F. Combustion studies by thermogravimetric analysis: 1. Coal oxidation. *Fuel* **1986**, *65*, 1546−1551.
(28) Li, C.; Suzuki, K. Kinetics of Perovskite catalyzed biomass tar combustion studied by thermogravimetry and differential thermal analysis. *Energy Fuels* **2009**, *23*, 2364−2369.
(29) Sutcu, H.; Piskin, S. Characterization and combustion kinetics of chars obtained from Loquat stones. *Combust. Sci. Technol.* **2009**, *181*, 264−273.
(30) Kök, M. V. Non-isothermal DSC and TG/DTG analysis of the combustion of Silopi asphaltites. *J. Therm. Anal. Calorim.* **2007**, *88*, 663−668.
(31) Ortega, A. Some successes and failures of the methods based on several experiments. *Thermochim. Acta* **1996**, *284*, 379−387.
(32) Maciejewski, M. Thermal analysis and kinetic concepts of solid-state reactions. *J. Therm. Anal. Calorim.* **1988**, *33*, 1269−1277.
(33) Criado, J. M.; Morales, J.; Rives, V. Computer kinetic analysis of simultaneously obtained TG and DTG curves. *J. Therm. Anal. Calorim.* **1978**, *14*, 221−228.
(34) Criado, J.; Gonzalez, M.; Ortega, A.; Real, C. Some considerations regarding the determination of the activation energy of solid-state reactions from a series of isothermal data. *J. Therm. Anal. Calorim.* **1984**, *29*, 243−250.
(35) Vyazovkin, S.; Dollimore, D. Linear and Nonlinear Procedures in Isoconversional Computations of the Activation Energy of Nonisothermal Reactions in Solids. *J. Chem. Inf. Comput. Sci.* **1996**, *36*, 42−45.
(36) Friedman, H. L. Kinetics of thermal degradation of char-forming plastics from thermogravimetry. Application to a phenolic plastic. *J. Polym. Sci., C: Polym. Symp.* **1964**, *6*, 183−195.
(37) Ozawa, T. Estimation of activation energy by isoconversion methods. *Thermochim. Acta* **1992**, *203*, 159−165.
(38) Flynn, J. H.; Wall, L. A. General treatment of the thermogravimetry of polymers. *J. Res. Natl. Bur. Stand., A: Phys. Chem.* **1966**, *70A*, 487−523.
(39) Hu, R. Z.; Shi, Q. Z. *Thermal analysis kinetics*; Science Press: Beijng, 2001.
(40) Doyle, C. D. Estimating isothermal life from thermogravimetric data. *J. Appl. Polym. Sci.* **1962**, *6*, 639−642.
(41) Zhang, L.; Binner, E.; Qiao, Y.; Li, C.-Z. In situ diagnostics of Victorian brown coal combustion in $O_2/N_2$ and $O_2/CO_2$ mixtures in drop-tube furnace. *Fuel* **2010**, *89*, 2703−2712.
(42) Arias, B.; Pevida, C.; Rubiera, F.; Pis, J. J. Effect of biomass blending on coal ignition and burnout during oxy-fuel combustion. *Fuel* **2008**, *87*, 2753−2759.
(43) Várhegyi, G.; Szabó, P.; Jakab, E.; Till, F.; Richard, J.-R. Mathematical modeling of char reactivity in Ar−$O_2$ and $CO_2$−$O_2$ mixtures. *Energy Fuels* **1996**, *10*, 1208−1214.
(44) Liu, H.; Zailani, R.; Gibbs, B. M. Comparisons of pulverized coal combustion in air and in mixtures of $O_2/CO_2$. *Fuel* **2005**, *84*, 833−840.
(45) Shaddix, C. R.; Molina, A. Particle imaging of ignition and devolatilization of pulverized coal during oxy-fuel combustion. *Proc. Combust. Inst.* **2009**, *32*, 2091−2098.
(46) Alonso, M. J. G.; Borrego, A. G.; Alvarez, D.; Parra, J. B.; Menéndez, R. Influence of pyrolysis temperature on char optical texture and reactivity. *J. Anal. Appl. Pyrolysis* **2001**, *58*−*59*, 887−909.
(47) Riaza, J.; Álvarez, L.; Gil, M. V.; Pevida, C.; Pis, J. J.; Rubiera, F. Effect of oxy-fuel combustion with steam addition on coal ignition and burnout in an entrained flow reactor. *Energy* **2011**, *36*, 5314−5319.
(48) Murphy, J. J.; Shaddix, C. R. Combustion kinetics of coal chars in oxygen-enriched environments. *Combust. Flame* **2006**, *144*, 710−729.
(49) Demir, I.; Hughes, R. E.; DeMaris, P. J. Formation and use of coal combustion residues from three types of power plants burning Illinois coals. *Fuel* **2001**, *80*, 1659−1673.
(50) Jak, E.; Degterov, S.; Hayes, P. C.; Pelton, A. D. Thermodynamic modelling of the system $Al_2O_3$−$SiO_2$−CaO−FeO−$Fe_2O_3$ to predict the flux requirements for coal ash slags. *Fuel* **1998**, *77*, 77−84.
(51) Hatt, R. M.; Bull, D. L. In *Mineral matter and ash deposition from coal*; Bryers, R. W., Vorres, K. S., Eds.; Engineering Foundation: New York, 1990.
(52) Kakali, G.; Perraki, T.; Tsivilis, S.; Badogiannis, E. Thermal treatment of kaolin: the effect of mineralogy on the pozzolanic activity. *Appl. Clay Sci.* **2001**, *20*, 73−80.
(53) Mitchell, R. S.; Gluskoter, H. J. Mineralogy of ash of some American coals: variations with temperature and source. *Fuel* **1976**, *55*, 90−96.